Article

pubs.acs.org/Biomac

Cationic Copolymerization of 3,3-Bis(hydroxymethyl)oxetane and Glycidol: Biocompatible Hyperbranched Polyether Polyols with High Content of Primary Hydroxyl Groups

Eva-Maria Christ,[†,‡] Dominika Hobernik,[§] Matthias Bros,[§] Manfred Wagner,[∥] and Holger Frey*[,†,‡]

[†]Institute of Organic Chemistry, Johannes Gutenberg-University Mainz, Duesbergweg 10-14, D-55128 Mainz, Germany

[‡]Graduate School Materials Science in Mainz (MAINZ), Staudingerweg 9, D-55128 Mainz, Germany

[§]Department of Dermatology, University Medical Center of the Johannes Gutenberg-University, Langenbeckstrasse 1, D-55131 Mainz, Germany

[∥]Max Planck Institute for Polymer Research, Ackermannweg 10, D-55128 Mainz, Germany

Supporting Information

ABSTRACT: The cationic ring-opening copolymerization of 3,3-bis(hydroxymethyl)oxetane (BHMO) with glycidol using different comonomer ratios (BHMO content from 25 to 90%) and BF_3OEt_2 as an initiator has been studied. Apparent molecular weights of the resulting hyperbranched polyether copolymers ranged from 1400 to 3300 g mol^{-1} (PDI: 1.21−1.48; method: SEC, linear PEG standards). Incorporation of both comonomers is evidenced by MALDI-TOF mass spectroscopy. All hyperbranched polyether polyols with high content of primary hydroxyl groups portray good solubility in water, which correlates with an increasing content of glycerol units. Detailed NMR characterization was employed to elucidate the copolymer microstructures. Kinetic studies via FTIR demonstrated a weak gradient-type character of the copolymers. MTT assays of the copolymers (up to 100 μg mL^{-1}) on HEK and fibroblast cell lines (3T3, L929, WEHI) as well as viability tests on the fibroblast cells were carried out to assess the biocompatibility of the materials, confirming excellent biocompatibility. Transfection efficiency characterization by flow cytometry and confocal laser microscopy demonstrated cellular uptake of the copolymers. Antiadhesive properties of the materials on surfaces were assessed by adhesion assays with fibroblast cells.

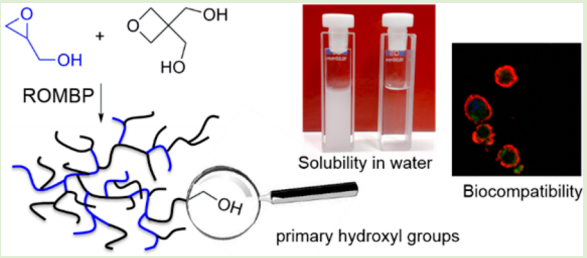

INTRODUCTION

Poly-3,3-bis(hydroxymethyl)oxetane (PBHMO) obtained from the cationic polymerization of bis(hydroxymethyl)oxetane (BHMO) is a hardly investigated polymer, which can be attributed to its poor solubility in common solvents. The BHMO monomer is available via a facile one-step synthesis that relies on the inexpensive starting materials pentaerythritol and diethyl carbonate.[1] The linear PBHMO structure, synthesized from silyl-protected BHMO followed by deprotection of the polymer, is an unusual material, as it exhibits a high melting point (314 °C) and possesses numerous hydroxyl groups that offer the possibility to postfunctionalize the material.[1] In the pioneering work regarding this material, Vandenberg et al. also introduced the synthesis of branched PBHMO in 1989.[1] BHMO, which represents a latent AB_3 monomer, can directly be (homo)polymerized, leading to strongly branched structures.[2] By replacing one of the two hydroxyl groups of BHMO with an alkyl chain, the solubility of the resulting polymer can be improved in a few organic solvents (e.g., pyridine or cresol).[3] Furthermore, the solubility of hyperbranched polyoxetanes increases upon etherification of one of the two hydroxyl groups of BHMO with an alkyl chain, which leads to a latent AB_2-type monomer structure.[4]

Hyperbranched (*hb*) polymers show lower viscosity, improved solubility, and nearly no entanglements in contrast to their linear analogues, due to their three-dimensional structure.[5−13] An intensely studied hyperbranched polymer is *hb*polyglycerol (*hb*PG) that can be prepared in a controlled ring-opening multibranching polymerization (ROMBP) by slow addition of glycidol to a partially deprotonated, hydroxyl-functional initiator molecule. Its biocompatibility, chemical stability and inertness under biological conditions has been extensively studied and exploited by several groups.[14−20] Hyperbranched polyglycerol possesses excellent biocompatibility and can be applied for a variety of biomedical purposes.[14,21,22] *hb*PG is commonly prepared by anionic ring-opening polymerization of glycidol.

Hyperbranched polyoxetanes are promising materials because of their facile synthesis via cationic ring-opening polymerization.[2,23−28] Moreover, the presence of merely primary hydroxyl groups in *hb*PBHMO can be synthetically advantageous in comparison to polyglycerol, which exhibits a

Received: July 15, 2015
Revised: September 9, 2015
Published: September 10, 2015

DOI: 10.1021/acs.biomac.5b00951
Biomacromolecules 2015, 16, 3297−3307

Scheme 1. Synthesis of Random Copolymers of Glycidol and BHMO by Cationic Ring-Opening Copolymerization (ROMBP: Ring-Opening Multibranching Polymerization)

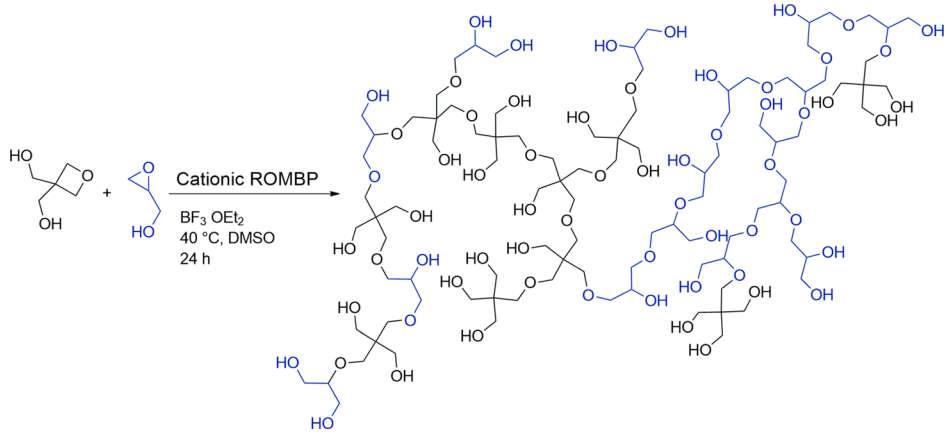

mixture of primary and secondary hydroxyl groups that are less reactive for further derivatization. The uniform reactivity of hyperbranched polyoxetanes has been exploited for further functionalization in several works to obtain well-defined structures and architectures, for example, for hyperbranched ionic liquids.[29−31] Additionally, hyperbranched polyoxetanes are well-known for their high chemical stability and inertness under oxidative conditions.[29] Hence, hyperbranched polyoxetanes have attracted increasing attention in recent years.[13,32−34] Unfortunately most of the reported hyperbranched polyoxetanes are hydrophobic and are only soluble in a very limited number of solvents.[23] To capitalize on the interesting properties of hyperbranched polyoxetanes, while enlarging the number of possible applications, copolymerization of 3-ethyl-3-hydroxymethyloxetane (EHO)[35] or 3-methyl-3-hydroxymethyloxetane (MHO)[11] with glycidol has been carried out. In a few works, EHO has been copolymerized with ethylene oxide.[36−38] In order to increase the number of branching units and hydroxyl groups in PEHO and PMHO, BHMO was used as a cyclic AB_3 comonomer in a few works.[1,2,39,40]

The cationic polymerization of glycidol was pioneered by Dworak et al. in two important works.[15−61] The authors demonstrated that apparent molecular weights up to 10 000 g mol^{-1} and branched polymers can be obtained, albeit without control of the molecular weights like in the anionic ROP. This is due to the concurrence of two different polymerization mechanisms, the active chain end (ACE) and active monomer (AM) mechanism in the cationic ring-opening polymerization, which was first described by Dworak et al. in 1994[61] and in 2001 for oxetanes,[26] as well as in various further publications.[41,63]

In the current work, we have studied the cationic random copolymerization of BHMO with glycidol (Scheme 1). We demonstrate that the combination of these cyclic latent AB_3 and AB_2 monomers results in hyperbranched polyether polyols with a large number of primary hydroxyl groups. Their solubility in water and the thermal characteristics of the resulting polyether polyols have been studied with respect to the comonomer ratio. Comprehensive characterization of all polymers via MALDI-ToF mass spectrometry, NMR spectroscopy, size exclusion chromatography (SEC), IR spectroscopy, and differential scanning calorimetry (DSC) has been carried out. To investigate biocompatibility of the materials, MTT assays, viability tests, as well as transfection efficiency analysis and confocal laser microscopy were conducted. Finally, adhesion assays were performed on surfaces to explore cell-repellent properties of the copolymers.

EXPERIMENTAL SECTION

Materials. All reagents were purchased from Acros Organics or Sigma-Aldrich and were used as received, unless otherwise stated. Anhydrous DMSO and boron trifluoride etherate were stored over molecular sieves prior to use. Column chromatography was performed on silica gel (particle size 63−200 μm, Merck, Darmstadt, Germany). Deuterated DMSO-d_6 and pyridine-d_5 were purchased from Deutero GmbH.

Instrumentation. ^{1}H NMR (300 and 400 MHz) and ^{13}C NMR spectra (75 and 100.6 MHz) were recorded on a Bruker AC300, Bruker AC400, Avance III HD 300 (300 MHz, 5 mm BBFO-head with z-gradient and ATM, B-ACS 60 sample changer) with Open-Access-Automation, Avance II 400 (400 MHz, 5 mm BBFO-head with z-gradient and ATM, SampleXPress 60 sample changer) with Open-Access-Automation, or Avance III HD 400 (400 MHz, 5 mm BBFO-SmartProbe with z-gradient and ATM, SampleXPress 60 sample changer), respectively, and were referenced internally to residual proton signals of the deuterated solvents. The ^{1}H NMR experiments for kinetic studies were acquired with a 5 mm BBFO z-gradient probe on the 500 MHz Bruker AVANCE III system. For a proton spectrum, 64 transients were used with a 10.6 μs long 90° pulse and 10 000 Hz spectral width together with a recycling delay of 10 s. For the ^{13}C NMR kinetic measurements 32 scans were used with a relaxation delay of 30 s (90° pulse: 13.2 μs, spectra width 30 000 Hz). The temperature was kept at 298.3 K and calibrated with a standard ^{1}H methanol NMR sample using the topspin 3.2 software (Bruker). Control of the temperature was realized with a VTU (variable temperature unit) and an accuracy of ±0.1 K. For size exclusion chromatography (SEC) measurements in dimethylformamide (DMF), a PU 1580 pump, an auto sampler AS1555, a UV-detector UV 1575 (detection at 254 nm), and a RI-detector RI 1530 from JASCO were used. Columns (MZ-Gel SDplus 10^2 Å and MZ-Gel SDplus 10^6 Å) were obtained from MZ-Analysentechnik. Calibration was carried out with polyethylene glycol (PEG) standards purchased from Polymer Standard Services (PSS). MALDI-ToF MS measurements were performed on a Shimadzu Axima CFR MALDI-TOF mass spectrometer using dithranol (1,8,9-trishydroxyanthracene) or CHCA (α-cyano-4-hydroxycinnamic acid) as a matrix. The samples were prepared from pyridine and ionized by adding lithium chloride or potassium trifluoro acetate. DSC measurements were carried out on a PerkinElmer DSC 8500 instrument in the temperature range of −80 to 50 °C, using heating rates of 10 K min^{-1} under nitrogen. Contact angle measurements were performed on a Dataphysics Contact Angle System OCA apparatus using water as an interface agent.

DOI: 10.1021/acs.biomac.5b00951
Biomacromolecules 2015, 16, 3297−3307

Table 1. Characterization Data for Copolymers with Different Ratios of 3,3-Bis(hydroxymethyl)oxetane (BHMO) and glycidol (G)

sample[a]	$[BHMO]_0/[G]_0$	M_n/g·mol^{-1}[b]	PDI[b]	T_g[c]	yield (%)[d]
P($BHMO_{0.25}$-*co*-$G_{0.75}$)	20:80	1400	1.33	−41	68.7
P($BHMO_{0.35}$-*co*-$G_{0.65}$)	30:70	2000	1.32	−41	62.5
P($BHMO_{0.39}$-*co*-$G_{0.61}$)	40:60	3300	1.48	−27	51.5
P($BHMO_{0.60}$-*co*-$G_{0.40}$)	50:50	2100	1.29	−23	73.9
P($BHMO_{0.61}$-*co*-$G_{0.39}$)	60:40	3000	1.21	−22	55.2
P($BHMO_{0.66}$-*co*-$G_{0.34}$)	70:30	2100	1.40	−12	66.4
P($BHMO_{0.80}$-*co*-$G_{0.20}$)	80:20	3300	1.41	−14	84.3
P($BHMO_{0.91}$-*co*-$G_{0.09}$)	90:10	2000	1.35	4	74.2

[a]Determined by IG ^{13}C NMR. [b]Determined by SEC in DMF vs PEG standards after functionalization with trifluoroacetic anhydride. [c]Determined by DSC, second heating cycle. [d]Determined by weight, after precipitation twice in ice-cold diethyl ether.

Synthetic Procedures. *Synthesis of 3,3-Bis(hydroxymethyl)-oxetane (BHMO).* BHMO was synthesized as described in the literature.[1] Briefly, pentaerythritol (200 g, 1.47 mol), diethylcarbonate (220 mL, 1.64 mol) and potassium hydroxide (0.3 g, 7.5 mmol) in ethanol (25 mL) were refluxed under argon atmosphere for 19 h. After removal of ethanol by distillation and cooling to room temperature, potassium hydroxide (0.23 g) dissolved in ethanol (20 mL) was added. (0.019 mbar) The crude product was obtained by distillation *in vacuo* (1.9×10^{-2} mbar, 98.9 g, 0.84 mol, yield: 62%, Lit.:[1] 40%). ^1H NMR (300 MHz, DMSO-d_6): δ (ppm) = 4.75 (t, 2H, J = 15 Hz, $-CH_2OH$), 4.54 (s, 4H, $-CH_2OH$), 4.27 (s, 4H, $-CH_2O$-).

Representative Procedure for the Synthesis of Hyperbranched Polyoxetane Copolymers. BHMO was dissolved in DMSO at 40 °C under argon atmosphere. Glycidol was added via syringe, followed by addition of boron trifluoride etherate (1 mol % of BHMO) via syringe. After 24 h, the polymerization was quenched with pyridine. The product was dissolved in 0.5 mL of pyridine and precipitated twice in ice-cold diethyl ether. The polymer was dried in vacuo at 90 °C for 2 d (yields: 52−85%). ^1H NMR (300 MHz, DMSO-d_6): δ (ppm) 6.87 (s, $-OH$), 4.79 (m, $-CH_2OH$), 4.20 (m, $-CH_2O-$).

Functionalization with Trifluoroacetic Anhydride (TFAA). An amount of 100 mg of the respective copolymer was dissolved in 5 mL of trifluoroacetic anhydride under argon atmosphere and refluxed for 8 h. The solution was cooled to room temperature, and trifluoroacetic anhydride was removed in vacuo. The product was dried under reduced pressure at 50 °C for 8 h (yield: 89%). ^1H NMR (300 MHz, DMSO-d_6): δ (ppm) 5.13−4.50 (m, $-CH_2OH$), 4.19−3.74 (m, $-CH_2O-$).

Labeling P($BHMO_{0.75}$-*co*-$G_{0.25}$) with Alexa 488. P($BHMO_{0.75}$-*co*-$G_{0.25}$) was synthesized, followed by subsequent derivatization with propargyl bromide as reported elsewhere.[53,64] Next, 100 mg of P($BHMO_{0.75}$-*co*-$G_{0.25}$) and Alexa 488 (5 equiv) were dissolved in 5 mL of dry DMSO, and a catalytic amount of Hünig's base was added. The mixture was degassed by three freeze−pump−thaw cycles, and $CuSO_4 \cdot 5H_2O$ (0.3 mol % per alkyne) and sodium ascorbate (0.6 mol % per alkyne) were added. The reaction was stirred at 50 °C for 48 h and then exposed to air.[54] The functionalized polymers were purified via dialysis in DMSO at room temperature for 1 week, and the solvent was changed every 12 h. After this procedure, the solvent was evaporated under reduced pressure at 90 °C for 4 days.

MTT Assays. Cytotoxic effects of polymer treatment were measured by MTT assay (Promega, Heidelberg, Germany). To this end, cells of fibroblast lines (3T3:10^4; L929, WEHI: each 5×10^3) were seeded in wells (100 μL) of 96-well cell culture-treated plates. On the next day, polymer was applied to triplicates at different concentrations up to 100 μg mL^{-1} as indicated. Samples treated with the cytotoxic agent DMSO up to 10% served as negative controls. After 24 h, metabolic activity of the cells was assessed by addition of MTT substrate/stop solution, followed by assessment of formazan production in an ELISA plate reader as recommended by the manufacturer.

Viability Tests. To assess cytotoxic properties of polymer on single cell level, fibroblasts (3T3: 1.2×10^5; L929, WEHI: each 4×10^4) were seeded in wells (800 μL) of 12 well cell culture-treated plates. On the next day, polymer was applied in parallel assays at 10 or 100 μg mL^{-1}. Samples left untreated or treated with DMSO at cytotoxic concentrations (3T3: 5 %; L929, WEHI: each 2.5 %) served as controls. After 24 h, cells were harvested, incubated with Annexin V Alexa Fluor (AF) 647 (Biolegend, San Diego, CA) and Fixable Viability Dye (FVD) eFluor 450 (affymetrix/ebioscience, San Diego, CA) and assayed by flow cytometry (FACSCanto; BD Biosciences, San Jose, CA) using FlowJo software (Ashland, OR) for subsequent analysis. Debris was gated out in the FSC/SSC plot, and fluorescence intensities of cells were determined. Annexin V^- FVD^- cells are alive, Annexin V^+ FVD^- cells are apoptotic, FVD^+ Annexin V^- cells are necrotic, and Annexin V^+ FVD^+ cells may constitute a mixture of late apoptotic/necrotic cells.

Transfection Efficiency. Cellular engagement of the polymers was monitored by flow cytometry. Fibroblasts were seeded as described above for assessment of viability. On the subsequent day, AF488-labeled polymer was applied in parallel assays at 10 or 100 μg mL^{-1}. For dialysis in DMSO, the dialysis bags or Dial D-Clean-MWCO 1000′ (Orange Scientific) were utilized. Cells were harvested after 6 and 24 h, respectively, and were analyzed as described above to detect $AF488^+$ cells.

Adhesion Assay. To assess potential antiadhesive properties of the polymer, first the sample P($BHMO_{0.9}$-*co*-$G_{0.1}$) was provided into wells of untreated 96-well plates. Polymer PS_{27}-(AGE)-$PE0_{130}$ with known repellant activity served as an internal control, and PBS buffer as a solvent control. The wells were treated with the copolymer by dropping the respective aqueous copolymer solution onto the well plates, followed by removal of the water under reduced pressure for 48 h. Cells of fibroblast lines (3T3: 4×10^4; L929, WEHI: each 2×10^4) were seeded in the wells (100 μL) of the pretreated 96-well plates in triplicate. On the next day, the wells were washed to remove unbound cells. The number of adherent cells was monitored by MTT assay as described above.

Confocal Laser Scanning Microscopy (CLSM). Cellular uptake of polymer was monitored by CLSM. To this end, cells (3T3: 5×10^4; L929, WEHI: each 3×10^4) were seeded in Chamber Slides (Thermo Fisher Scientific, Waltham, MA). On the next day, AF488-labeled polymer was applied (100 μg mL^{-1}). The following day, the chamber slides were washed, and the samples were incubated with DAPI (Sigma-Aldrich, Deisenhofen, Germany) to stain cell nuclei (blue) and with Cell Mask Orange (Thermo Fisher Scientific) to stain cell membranes (red). Unbound dyes were washed off. Samples were assayed using a TCS SP5 instrument (Leica, Wetzlar, Germany), and analyzed using IMAGEJ software (1.49o, NIH Bethesda, MD).

RESULTS AND DISCUSSION

Synthesis and Characterization of Hyperbranched Polyethers. Copolymers of 3,3-bis(hydroxymethyl)oxetane (BHMO) and glycidol were synthesized by cationic random ring-opening copolymerization in one step (Scheme 1), using boron trifluoride etherate as a catalyst. A series of copolymerizations of BHMO and glycidol was conducted,

DOI: 10.1021/acs.biomac.5b00951
Biomacromolecules 2015, 16, 3297−3307

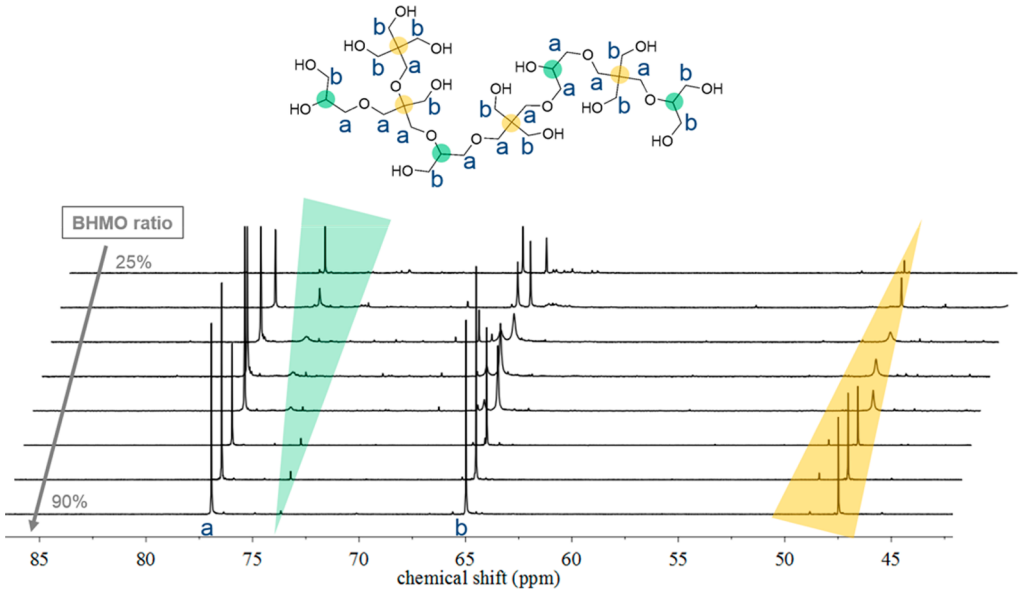

Figure 1. IG ^{13}C NMR spectra (100 MHz, pyridine-d_5) of copolymers of BHMO and glycidol with different comonomer ratios (BHMO ratio in the range of 25−90%; green, tertiary carbon atoms of glycidol units; yellow, quaternary carbon atoms of BHMO units).

employing systematically varied comonomer ratios, ranging from 20 to 90% BHMO content. All copolymerizations shown in Table 1 were conducted at 40 °C for 24 h. Complete conversion of the monomers after this reaction time is supported by ^{1}H NMR (SI Figure 14). In all cases, colorless, highly viscous products were obtained in yields ranging from 52 to 85% (Table 1). The colorless appearance of the products distinguishes the polymers from *hb*PG prepared by AROP that is often obtained as a slightly yellow or brownish material. Apparent molecular weights were determined by SEC in DMF vs PEG standards after functionalization of the hydroxyl groups of the hyperbranched polymers with trifluoroacetic anhydride. As in other hyperbranched polyols, these values cannot be taken as absolute molecular weights and are likely to be underestimated.[62] Characterization data for all materials are listed in Table 1.

The compact, globular structure of hyperbranched polymers often leads to strongly underestimated values of the molecular weights. Interaction of the large number of hydroxyl groups with the SEC columns can have additional impact on the molecular weights measured by SEC. Accordingly, substitution of the hydroxyl groups is therefore indispensable to improve SEC characterization, leading to a better solubility of the copolymers in the solvent.[4,29,31,42] The transformation of the hydroxyl groups with trifluoroacetic anhydride has been investigated by ^{1}H NMR, as detailed in the Supporting Information (SI Figure 1). The signal belonging to the hydroxyl groups at 6.87 ppm disappears completely after derivatization. From these results, successful functionalization of the hydroxyl groups of the copolymers is evident. The measured molecular weights after functionalization ranged from 1400 to 3300 g mol^{-1}, with polydispersities between 1.21 and 1.48 (SEC in DMF with linear PEG standards, SI Figure 2), which is in good agreement with other hyperbranched polyoxetane homopolymers synthesized by cationic ring-opening polymerization.[2,23,24,27,39] Due to the AB_3 structure of BHMO, copolymers with a high BHMO content possess a higher number of hydroxyl groups in comparison to polyglycerol as well as other hyperbranched polyoxetane homopolymers based on cyclic AB_2 monomers reported to date. The molecular weights of the polymers are limited. Hydrogen bonding of the termini may contribute to lowering of the reactivity of the hydroxyl groups.[43] Nevertheless, molecular weights and polydispersities are in the same range as values obtained for the anionic ROP of glycidol, if no slow monomer addition is employed.[44] However, in contrast to this approach, molecular weights by cationic ROMBP are not controllable.

MALDI-ToF mass spectra of the copolymers support the results of the SEC, even though molecular weights by MALDI-ToF are most likely underestimated, due to the "mass discrimination effect".[44] In the MALDI-ToF spectra of the copolymers the distribution maxima are generally observed at around 3.500 g mol^{-1}, which indicates considerably higher M_n than this value, considering the well-known mass discrimination effect. MALDI-ToF results also confirm the successful copolymerization of glycidol and BHMO, since the respective linear combinations of both units are present in the mass spectra. A detailed assignment of all signals in the spectra of three exemplary copolymers with varied monomer ratio (from 20 to 80% BHMO incorporation), observed via MALDI-ToF MS, is given in the Supporting Information (see SI Figures 3−5).

It is an important issue, whether the highly strained epoxide monomer glycidol and the less strained oxetane BHMO react at a similar rate in the cationic ring-opening process. Inverse gated (IG) ^{13}C NMR spectroscopic characterization of the copolymers suggests comonomer contents close to the composition of the monomer mixtures employed (Table 1). IG ^{13}C NMR spectroscopy is a frequently employed method to determine the composition of copolymers,[54,26,42,4] for which other spectroscopic methods do not yield reliable results. The quaternary carbon atoms of the BHMO units (Figure 1, 47.6 ppm) exhibit a distinct chemical shift that differs from the dendritic carbon atoms of the glycidol units (Figure 1, 73.7−74.9 ppm). An example of the chemical structure of the polymers is given in Figure 1. Obviously there is a large variety of possible dendritic, semidendritic, linear, and terminal units (see SI Figures 6 and 7). Because of a variety of possible

DOI: 10.1021/acs.biomac.5b00951
Biomacromolecules 2015, 16, 3297−3307

neighboring units, broad signals are observed, for example, for the resonances belonging to CH_2 groups at 63−66 ppm.

The signal assignment of the ^{13}C NMR spectra is supported by DEPT (SI Figures 6 and 7) and HSQC NMR measurements (Figure 2 and SI Figures 8−11). It is in line with results

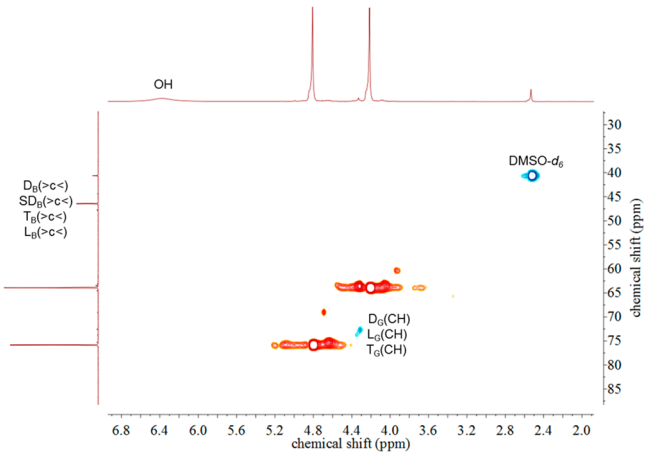

Figure 2. HSQC NMR spectrum of P($BHMO_{0.8}$-*co*-$G_{0.2}$) in DMSO-d_6. Blue signals belong to CH or CH_3 groups, and red signals to CH_2 groups.

reported by Xia et al. for copolymers of glycidol and 3-methyl-3-hydroxymethyloxetane.[45] In the IG ^{13}C NMR shown in Figure 1, the signals at 45−47 ppm are assigned to the quaternary carbon atom of the BHMO units. The signals of the tertiary carbon atoms (CH groups) of glycidol units are observed at 70−72 ppm. As the molar ratio of BHMO increases, the intensity of the signals of the quaternary carbon atom rises, as expected. The appearance of several signals stemming from the quaternary carbon atom is probably due to the polymer microstructure, that is, different possible neighboring units (glycidol or BHMO units). The relative quantity of BHMO can be calculated by comparing the signal intensities of the tertiary carbon atoms of the glycerol units with the signal intensity of the quaternary carbon atom of the BHMO units. Figure 2 shows the magnified HSQC of P($BHMO_{0.8}$-*co*-$G_{0.2}$). The signals of CH groups belonging to glycerol units are displayed in blue. No cross-relaxation is observed in the HSQC spectrum for the signal at 46.32 ppm. Therefore, this signal can be assigned to the quaternary carbon atoms of BHMO units. A detailed assignment of all signals is given in the Supporting Information (SI Figure 7).

The signals of the glycerol units of the copolymers in the ^{13}C NMR spectrum exhibit chemical shifts comparable to the pattern of polyglycerol obtained from the oxyanionic homopolymerization of glycidol. In the case of homopolymerization, typical signals between 79 and 82 ppm are observed, and the signal pattern and assignment is well-known.[16] Homopolymerization of BHMO would lead to an insoluble product in DMSO-d_6. It should be emphasized that no insoluble material, which would be indicative of PBHMO homopolymer, was observed either during workup of the reaction or in the NMR spectra.

In order to gain more detailed insight into the copolymerization kinetics and the resulting microstructure of the resulting copolymers, particularly with respect to the rates of incorporation of the two comonomers, ^1H NMR kinetic measurements have been performed for several days at room temperature. Different reactivities of the oxetane and the epoxide monomer structure might be expected due to the difference in ring strain (oxirane, 112 kJ mol^{-1}; oxetane, 106 kJ mol^{-1}).[46,47] Copolymerization of glycidol and BHMO can lead either to gradient or random copolymers, and gradient copolymer structures might be expected due to the higher reactivity of oxiranes compared to oxetanes. Figure 3 shows the ^1H NMR spectrum of a mixture of BHMO and glycidol (1:1) before initiation (b.i.), and six ^1H NMR spectra after initiation with 1 mol % boron trifluoride etherate in a time frame of 10 min to 72 h. In addition, the ^1H NMR spectrum of the resulting copolymer after termination and precipitation (a.p.) is displayed (top). The focus of this experiment was on the study of the conversion of both monomers at the early stages of the copolymerization. Therefore, the ^1H NMR kinetic study was conducted at room temperature, in contrast to the polymerizations at 40 °C shown in Table 1.

The conversion of glycidol can be calculated by plotting the intensity of the decreasing signals of the ring protons vs time. For this purpose, the integral of the multiplet at 2.99 ppm is set to 0% conversion. Complete conversion of glycidol (>98%) is

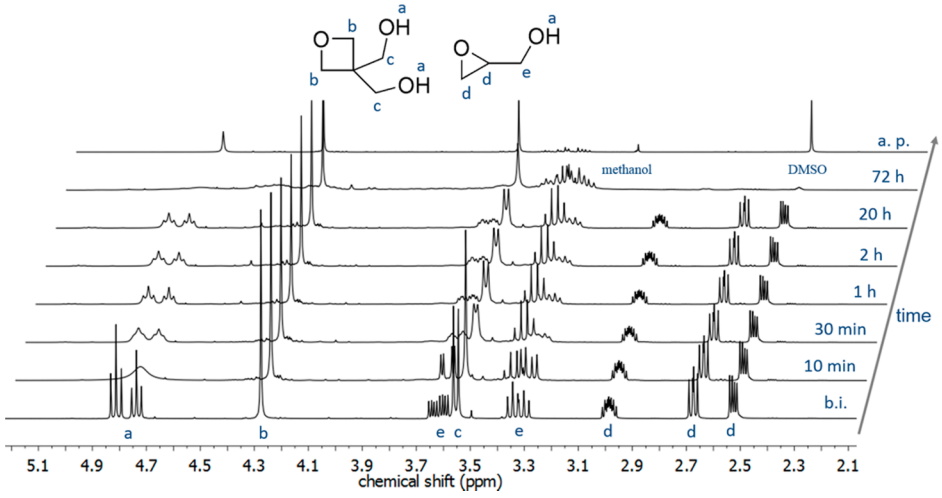

Figure 3. ^1H NMR spectra: kinetic study (300 MHz, DMSO-d_6) of the copolymerization of BHMO and glycidol at room temperature. b.i.: before initiation with boron trifluoride etherate. a.p.: after termination with methanol and precipitation in cold diethyl ether.

DOI: 10.1021/acs.biomac.5b00951
Biomacromolecules 2015, 16, 3297−3307

achieved after 3 days at room temperature. However, concurrently BHMO is incorporated into the hyperbranched polymer structure as well. Even 10 min after initiation a transformation of the signals at 4.27 ppm that stem from the oxetane ring and at 3.56 ppm for the hydroxymethyl groups is visible. Subsequently, both signals become broader and the doublet at 3.56 ppm changes to a multiplet. Furthermore, the change of the signal assigned to the hydroxyl groups of BHMO is similar to the change of the signal of the hydroxyl groups of glycidol, since both signals become broader and merge into one signal. Detailed analysis of the spectra provides qualitative information on the successful incorporation of both monomers (see also amplification of the spectra in SI Figure 24).

Besides ^{1}H NMR spectroscopy, ^{13}C NMR kinetics studies have been carried out (for detailed information on the kinetic studies, please see SI Figures 15 to 20 as well as SI Tables 1 and 2). Because of the long measuring times of IG ^{13}C NMR spectra in solvents, online ^{13}C NMR spectroscopy without solvent was utilized in this case. The polymerization of BHMO with glycidol at room temperature was started in the NMR tube immediately before measuring the first spectrum, followed by recording spectra every 3 min for 16 h. For initiation in bulk, 0.001 mol % of boron trifluoride etherate was applied. Unfortunately, without solvent the copolymerization proceeded within a few minutes. However, the spectra support the qualitative results of the ^{1}H NMR kinetics. With increasing time, the signals at 52.01 and 43.53 ppm that stem from glycidol decrease. A signal group at 67.3−72.5 ppm appears and increases, which is assigned to glycerol units and was utilized to determine the comonomer ratio (Figure 1, 73.7−74.9 ppm). The chemical shifts of signals that originate from BHMO do not vary significantly with increasing time. However, the incorporation of BHMO is indicated by a clear broadening of the signals at 75.04, 62.75, and 44.72 ppm that are due to BHMO.

By repeating the protocol with 6×10^{-4} mol % of initiator to decelerate the reaction rate, the onset and propagation of the polymerization can be observed in more detail. Regarding the signals of BHMO at 75.5, 63.2, and 45.1 ppm, chemical shifts are conspicuous with increasing time. This can be explained either by solvent effects, because of the changing viscosity with increasing amount of polymer or by conversion of the BHMO monomer. Due to the fact that the signals belonging to the glycerol units in the polymers do not feature significant alignment shifts in one direction with increasing reaction time, conversion of BHMO is confirmed. In summary, the ^{13}C NMR kinetic studies support the qualitative results of the ^{1}H NMR kinetics, which demonstrate incorporation of both monomers and thus successful copolymerization.

Unfortunately, the quantitation of the conversion of BHMO is not possible with NMR spectroscopy due to the indistinguishability of the chemical shifts of the monomer (^{1}H NMR: 4.22 and 3.55 ppm) and the polymer signals (^{1}H NMR: 4.59−4.06 and 3.87−3.49 ppm). Hence, the relative reactivity of the monomers BHMO and glycidol was investigated by IR spectroscopy as well. Polymerization was conducted in DMSO as a solvent at 40 °C with 1 mol % initiator. A total of 21 samples were retrieved (at time intervals from 5 to 180 min), terminated with methanol, and dried under reduced pressure. Figure 4 depicts the obtained spectra in the crucial region of 1200−800 cm^{-1}, together with the spectra of the monomers BHMO and glycidol (above) and the precipitated polymer (below). The polymerization was

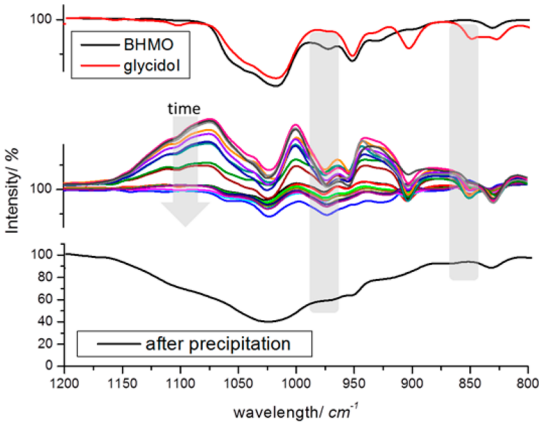

Figure 4. IR kinetics of the copolymerization of BHMO and glycidol (in the middle), the monomers above (red for glycidol and black for BHMO), and the precipitated polymer below (black).

terminated with methanol after 24 h, and the crude product was dried under reduced pressure at 90 °C for 2 days. By integration of the band at 840−860 cm^{-1} corresponding to glycidol and the band at 966−988 cm^{-1}, which corresponds to BHMO, the relative conversion can be calculated. The assignments of the bands to the monomers were possible by comparing the spectra with those of the monomers. In order to gain insight into the conversion rates, the gradients of the integral of these vibrations were compared (see SI Figures 21 and 22 and SI Tables 3−5). After subtracting the spectrum at the starting point, the normalized area of the vibrations attributed to glycidol decreases faster than the normalized area of the BHMO band (1.27/1 glycidol/BHMO; 56% glycidol and 44% BHMO conversion), supporting a weak gradient in monomer incorporation.

Diagrams of the gradient are given in SI Figure 22. The spectra of Figure 4 clearly demonstrate the conversion of both BHMO and glycidol, with increasing time (3 h). Furthermore, the weak gradient structure of the polymers is supported by IR spectroscopy.

Properties of the Hyperbranched Polyether Copolymers and Biocompatibility Studies. *Differential Scanning Calorimetry.* Differential scanning calorimetry (DSC) has been used to quantify the thermal properties of the copolymers of glycidol and BHMO. Table 1 lists the resulting glass transition temperatures (T_g), showing a clear trend with increasing content of BHMO units. With increasing amounts of BHMO in the copolymers, the T_g's increase from −41° (80% glycidol) to 4 °C (9% glycidol).

In comparison to hyperbranched PEHO, the glass transitions of the series of copolymers are considerably lower [T_g (PEHO): 40 °C[48]]. Also, PHMO exhibits higher glass transition temperatures [T_g (PHMO): 13 °C[45]]. To the best of our knowledge, linear PBHMO possesses the highest T_g of all polyether polyols with a T_g around 98 °C.[1] Besides, it is well-known that glass transitions of hyperbranched polyether copolymers are correlated to the comonomer ratio.[49] Hence, our results regarding the increase of T_g with increasing amounts of BHMO agree with expectation.

Contact Angle Measurements. Besides the investigation of the thermal behavior, contact angle measurements of water on P(BHMO-*co*-glycidol)-films have been carried out to assess surface properties of this material. In the subsection "Adhesion Assays" of this paper, deposition and surface properties play an

DOI: 10.1021/acs.biomac.5b00951
Biomacromolecules 2015, 16, 3297−3307

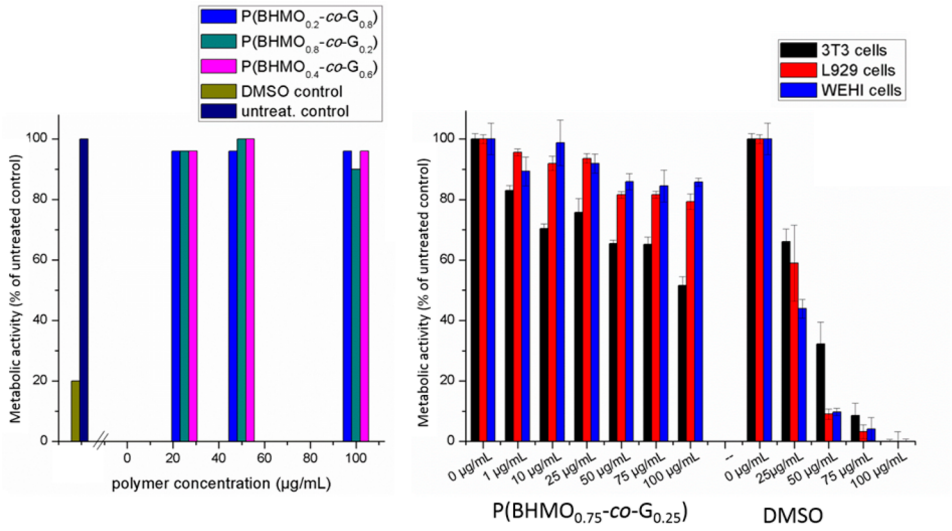

Figure 5. Left: MTT assay of HEK-293 cells for three copolymers with varied monomer ratio (from 20 to 80% BHMO). Right: MTT assay of three fibroblast cell lines (3T3 in black, L929 in red, and WEHI in blue). Incubation time of all assays: 24 h at room temperature.

important role. With increasing BHMO content in the copolymers, the materials showed increasingly hydrophobic behavior in solubility tests, although they possess numerous hydroxyl groups, which should contribute to low contact angles. Figure 23 of the Supporting Information shows the measured contact angles for the copolymers. Silicon wafers were coated using copolymer solutions in pyridine. Subsequently, pyridine was evaporated under reduced pressure at 90 °C for 48 h. With increasing amount of BHMO the contact angle increases from 4.8° for 20% BHMO units up to 34.1° for 100% BHMO units (PBHMO). The results mirror the content of BHMO, as expected.

Solubility. Copolymerization of BHMO with glycidol clearly leads to improved solubility in numerous common solvents; for example, P($BHMO_{0.5}$-*co*-$G_{0.5}$) is soluble in water, methanol, ethanol, HFIP, acetone, THF, DMF, DMSO, pyridine, triethylamine, ethyl acetate, and acetonitrile. In contrast, the hyperbranched PBHMO homopolymer is known to be poorly soluble in any solvent.[1] With increasing fraction of glycidol, the solubility of the copolymers in water increases significantly. Even with as little as 10% of glycidol units, the polymer is readily soluble in water (up to concentrations of 1 mg mL^{-1}). The improved solubility of polyoxetanes in water offers promise for various fields, ranging from biomedical applications to well-defined surface functionalization.

Biocompatibility: MTT Assays. By combining the widely studied polymer polyglycerol[19] with the hitherto not investigated material PBHMO, we aimed at a novel materials with good biocompatibility. It is well-known that hyperbranched polyglycerol shows excellent biocompatibility.[21] To investigate the biocompatibility of the novel PBHMO copolymers, cellular metabolic activity of HEK-293 cells (human embryonic kidney cells) was studied by MTT assay (see Figure 5, left) after incubation with several copolymers with varied BHMO/glycidol ratio for 24 h. Accordingly, the cytotoxicity of three copolymers with an amount of BHMO of up to 80% has been investigated. For this study, each copolymer was dissolved in phosphate-buffered saline and applied at three concentrations. The metabolic activity of untreated cells was set to 100%. Upon treatment with DMSO to induce cell death, the metabolic activity was reduced to 20%. Even at a rather high concentration of 100 $\mu g\ mL^{-1}$, all three copolymers showed no effect on metabolic activity. Consequently, copolymers of BHMO and glycidol can be considered to be highly biocompatible.

In contrast, polyoxetanes with alkoxy, bromomethyl, fluoroalkoxy, alkoxy-cycloalkyl, alkoxypolyoxyethylene, hydantoin, or quaternary ammonium side chains were patented for their antimicrobial behavior.[50] However, also without these peculiar substituents some polyoxetanes are known to be nonbiocompatible: Copolymers consisting of 3-ethyl-3-hydroxymethyloxetane (EHMO) and PEG possess low cytocompatibility for human dermal fibroblasts.[51] Exceptionally, a polymer concentration of up to 10 $\mu g\ mL^{-1}$ with a fraction of at most 17% of EHMO was observed to possess cell viability exceeding 80%.[51] Biocompatibility of PEHMO-PEG hydrogels to fibroblasts was demonstrated by MTT assay with a maximum concentration of the polymer of 10 $\mu g\ mL^{-1}$ as well.[38] Recently, no toxicity of a PEHMO-*g*-PEG polymer at a concentration up to 33 $\mu g\ mL^{-1}$ was demonstrated by luciferase assay.[52] However, there are only few studies concerning the biocompatibility of polyoxetanes. Moreover, most results are based on low polymer concentrations. To the best of our knowledge, no results for PBHMO or polymers with BHMO units related to their biocompatibility have been published to date.

To obtain further information on the biocompatibility of the copolymers, we carried out MTT assays with three fibroblast cell lines (3P3, L929 and WEHI cells). We chose these cell lines because of the known high sensitivity of fibroblasts in comparison to HEK-293 cells and because of their important role in wound healing processes. As a relevant copolymer, we deliberately chose P($BHMO_{0.75}$-*co*-glycidol$_{0.25}$) with a high amount of oxetane units and applied this in a range of concentrations of 1−100 $\mu g\ mL^{-1}$. The results of several experiments with different cell lines are summarized in Figure 5 (right diagram). In all assays regarding the copolymer the 3T3 cells (black columns) were clearly the most sensitive cells in comparison to L929 (red columns) and WEHI (blue columns) cells. At the highest copolymer concentration tested (100 $\mu g\ mL^{-1}$), the metabolic activity of 3T3 cells was 52%. For L929 cells, we observed 79% and for the WEHI cell line 86%.

DOI: 10.1021/acs.biomac.5b00951
Biomacromolecules 2015, 16, 3297−3307

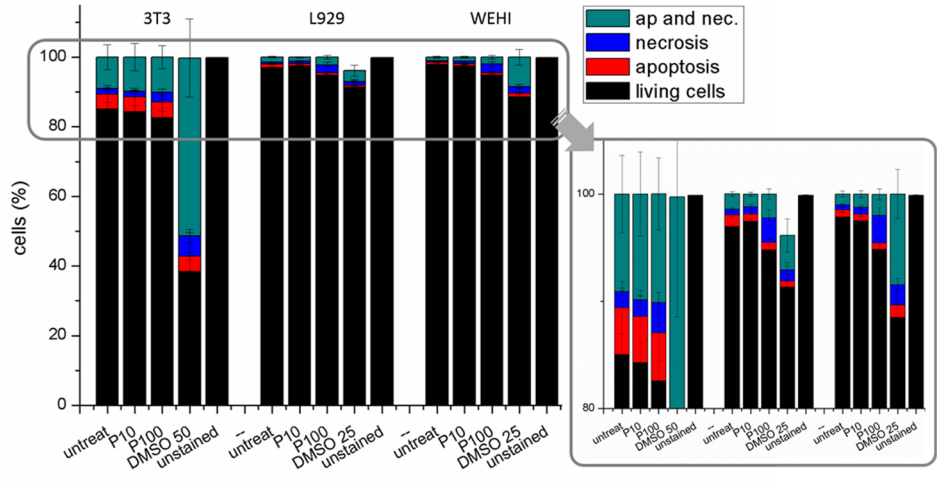

Figure 6. Viability tests by FACS analysis of fibroblast cells (3T3, L929, and WEHI) after incubation with P($BHMO_{0.75}$-*co*-$G_{0.25}$) for 24 h.

Scheme 2. Modification of P($BHMO_{0.75}$-co-$G_{0.25}$) with the Fluorescence Label Alexa 488 via Click Chemistry

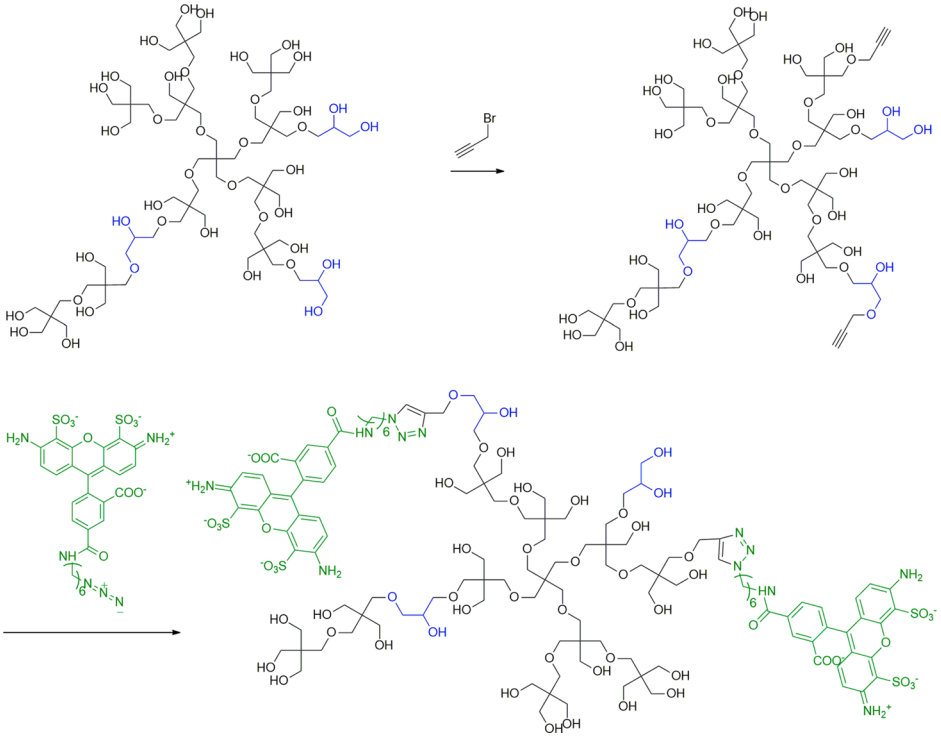

Summing up, these results show that the copolymer exerts only moderate effects on cellular metabolism, with the marked exception of 3T3 cells, supporting our results of the MTT assays using HEK cells.

Our results are comparable to the results of Xia et al. for copolymers of glycidol and the considerably less polar 3-methyl-3-hydroxymethyloxetane with similar concentrations.[45] However, copolymers in the work of Xia et al. were investigated with a maximum amount of the oxetane monomer of 35%, as determined from ^{13}C NMR spectra. Moreover, with increasing concentration of the polymers, cell viability for COS-7 cells decreased slightly.[45] This trend cannot be accredited by our results of the MTT assay on HEK cells.

In conclusion, copolymers of BHMO and glycidol exhibit high potential regarding their biocompatibility for both L929 and WEHI cells (even at a high concentration of 100 μg mL^{-1}), despite their high amount of ring-opened oxetane units (up to 80%).

Viability Tests. Regarding the cell line-dependent moderate (L929, WEHI) or stronger (3T3) decrease of the metabolic activity with increasing copolymer concentration, viability tests by FACS analysis have been performed. It is an important issue, whether the fibroblast cells died in response to incubation with copolymer, and, if so, whether this occurred because of necrosis or rather apoptosis.

To this end, fibroblast cells (3T3, L929 and WEHI cells) were incubated with the copolymer P($BHMO_{0.75}$-*co*-glycidol$_{0.25}$) for 24 h and FSC/SSC plots were utilized to investigate the size and granularity of the cells. Lower molecular weight particles, which may constitute cell debris, were gated out. Subsequently, FixViabDye/Annexin V plots for samples incubated with 10 μg mL^{-1} (P10) and 100 μg mL^{-1} (P100)

DOI: 10.1021/acs.biomac.5b00951
Biomacromolecules 2015, 16, 3297−3307

of copolymer solution, for untreated and unstained cells as well as for incubation with DMSO (negative control; 50 or 25 μg mL^{-1}), were used to assess rates of apoptotic and necrotic cells in each sample. This protocol was repeated four times. The results of these experiments are summarized in Figure 6.

The results show that with increasing polymer concentration the cell viability decreased slightly in case of L929 and WEHI cells, in accordance with a moderate decrease of cellular metabolic activity, as monitored by MTT assays. Again, 3T3 cells were the most sensitive cell line toward incubation with copolymer (100 μg mL^{-1}) with the lowest cell viability (83%) in contrast to L929 (91%) and WEHI cells (95%). These high viability values clearly underline the biocompatibility of the material. The zoom-in in Figure 6 (right panel) offers detailed information regarding the cause of cell death. For the 3T3 cells, apoptosis (Annexin V$^+$), late apoptosis (Annexin V$^+$7-AAD$^+$), and necrosis (Annexin V$^-$7-AAD$^+$) constitute the main cause of death. In the case of L929 and WEHI, late apoptosis and necrosis occurred at low extent only.

Transfection Efficiency Analysis and Confocal Laser Microscopy. Given the high biocompatibility of the polymer, we also assessed its transfection efficacy by flow cytometry.

For the transfection efficiency analysis, we functionalized some of the hydroxyl groups of the copolymer (P(BHMO$_{0.75}$-*co*-G$_{0.25}$) by attaching propargyl bromide after deprotonation of the polymer with sodium hydride. Subsequently, Alexa488 azide was attached as a fluorescence label via click chemistry[53,54] (see Scheme 2), as described in the Experimental Section. For purification, the functionalized polymers were purified via dialysis in DMSO for 1 week at room temperature. The solvent was changed every 12 h, and SEC measurements were carried out to ensure that neither unbound fluorescence label nor nonfunctionalized hyperbranched copolymer were present in solution at the end of this procedure. After this procedure, the solvent was evaporated under reduced pressure and at 90 °C for 4 days. The transfection efficiency analysis was conducted after incubation of 3T3, L929 and WEHI cells with labeled P(BHMO$_{0.75}$-*co*-G$_{0.25}$) at concentrations of 10 and 100 μg mL^{-1} for short (6 h) and longer (24 h) periods of time. Histograms of the mean FITC-A values (fluorescence signal of cell engaged copolymer) are summarized in Figure 7.

For all three fibroblast cell lines, the mean fluorescence values correlated with increasing incubation time with copolymer. This effect is even more distinctive for the higher concentration of 100 μg mL^{-1}. With regard to the untreated cells as well as to the cells treated with DMSO (solvent control), the mean fluorescence values of the cells incubated with 100 μg mL^{-1} of the labeled copolymer were clearly higher. This demonstrates that all three kinds of fibroblast cells interacted with the polymer.

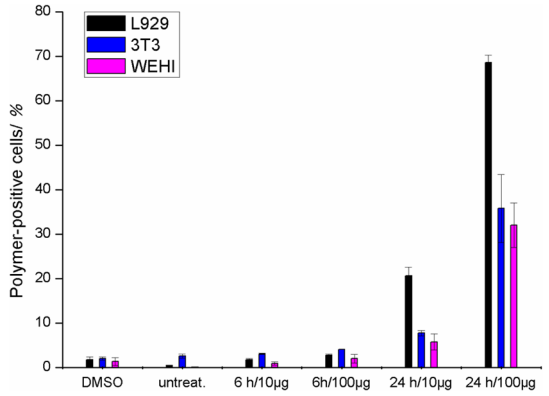

Figure 7. Polymer-positive cells (in %) after 6 and 24 h for three kinds of fibroblast cells after incubation with fluorescence labeled P(BHMO$_{0.75}$-*co*-G$_{0.25}$) and DMSO.

To evaluate potential cellular uptake of the polymer by the fibroblast cells (L929, WEHI and 3T3) confocal laser microscopy was carried out. For this purpose, cells were incubated with AF488-labeled P(BHMO$_{0.75}$-*co*-G$_{0.25}$) for 24 h, washed, and costained with DAPI (cell nuclei, blue) and Cell Mask Orange (cell membranes, red). Figure 8 illustrates images of L929 (left), WEHI (middle), and 3T3 cells. Polymer is visible in green.

For all three fibroblast cell lines, uptake of polymer into cells is clearly visible. In summary, both methods, the transfection efficiency analysis as well as the confocal laser microscopy, showed successfully that the living cells ingested the polymer. The observed uptake of the polymers into the cells offers potential for drug delivery systems.

Adhesion Assays. The novel copolymers with numerous hydroxyl groups permit postpolymerization transformation and possess a compact hyperbranched structure and tunable solubility. Their high compatibility with cells (HEK-939, WEHI, and L929 cells) provides a base for a possible application in surface functionalization: The hydroxyl groups might be utilized to covalently attach the polymer to a surface. To assess potential antiadhesive properties of the materials, adhesion assays have been carried out. As an internal control and comparison, we used a block copolymer with a short polystyrene block, enabling adhesion of the polymers to the wells, and a PEO block, which is known for its repellant activity to cells.[55] The synthesis of the internal control PS$_{27}$-(AGE)-PE0$_{130}$ is described in literature.[56]

Results are shown in Figure 9 for 3T3 (black), L929 (red), and WEHI (blue) cells on P(BHMO$_{0\text{-}9}$-*co*-G$_{0.1}$) (P1, Figure 9) in two quantities (1 and 10 μg) as well as with respect to the internal control PS$_{27}$-(AGE)-PE0$_{130}$ (P2). For both polymers, the cell-repellent effect increases with increasing quantity of polymer. Although the internal control shows a more significant cell repellency effect, the effect is clearly visible for the hyperbranched polyether polyol as well. The differences between the repellant effect of the two polymers are most probably related to the difference of the molecular weights (P(BHMO$_{0.9}$-*co*-G$_{0.1}$): M_n = 2000 g mol^{-1} and PS$_{27}$-(AGE)-PE0$_{130}$: M_n = 8500 g mol^{-1}). Nevertheless, the results underline the interesting properties of the materials for a wide range of applications. Further studies regarding biomedical application, including drug carrier systems, are in progress.

CONCLUSIONS

Hyperbranched aliphatic polyethers are interesting materials with potential applications in many different areas.[41,57,58] However, to date, polymers consisting of 3,3-bis-(hydroxymethyl)oxetane (BHMO) units have been hardly investigated, due to their low solubility both in organic solvents and aqueous solution. In this work, hyperbranched copolymers of BHMO as a latent AB$_3$ monomer with glycidol (latent AB$_2$ structure) have been introduced, which are readily soluble in organic solvents and water. The water-soluble copolymers of BHMO and glycidol studied consist of up to 90% of BHMO units. It is remarkable that as little as 10% of glycerol units in the copolymers render the materials water-soluble, in contrast

DOI: 10.1021/acs.biomac.5b00951
Biomacromolecules 2015, 16, 3297−3307

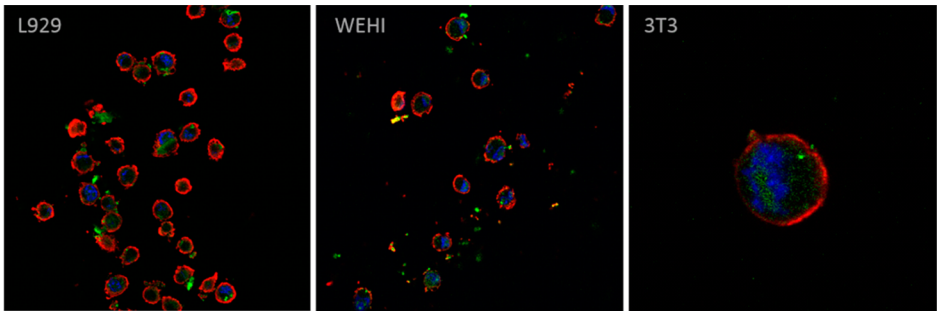

Figure 8. Confocal laser microscopy of fibroblast cells (L929, WEHI, and 3T3) after incubation with AF488-labeled P($BHMO_{0.75}$-*co*-$G_{0.25}$) for 24 h. Blue, cell nuclei; red, cell membranes; green, polymer.

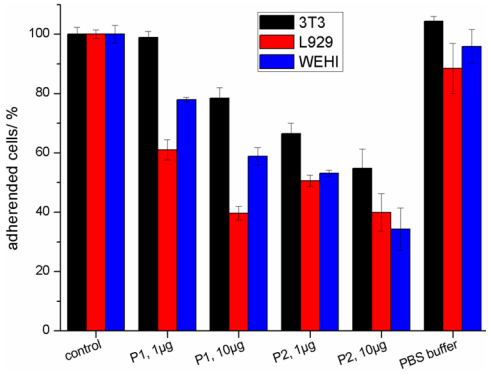

Figure 9. Adhesion assay of fibroblast cells (3T3, L929, and WEHI) on P($BHMO_{0\text{-}9}$-*co*-$G_{0.1}$) and the internal control PS_{27}-(AGE)-$PE0_{130}$ in two quantities each, as well as the control without polymer layer and the polymer solvent PBS buffer.

to the PBHMO homopolymer, which is an intractable material. Comparing the new copolymers to the established hyperbranched polyglycerol, which shows good solubility in water as well, the new structures possess almost exclusively primary hydroxyl groups. Keeping in mind the frequently applied capping of polyethers with ethylene oxide units to establish primary hydroxyl groups to enhance reactivity,[59] it is evident, that primary hydroxyl groups are desirable, since they are 3 to 3.3 times more reactive than secondary hydroxyl groups in the reaction with aromatic isocyanate groups and even up to 21 times more reactive in catalyzed reactions.[60]

Apparent molecular weights (SEC, MALDI-ToF) of the copolymers obtained by cationic ring-opening copolymerization were in the range of 1400−3300 g mol^{-1} and therefore comparable to molecular weights of several polyglycerols prepared by anionic ROP; however, in contrast the molecular weight of the new copolymers is not controllable by cationic ring-opening polymerization.

The BHMO-based copolymers show biocompatibility to HEK-293 as well as fibroblast (L929 and WEHI) cell lines, which renders them interesting for biomedical applications. The observed cellular uptake of the polymers is promising for drug delivery systems. In addition, the materials show cell repellant properties at surfaces, which are promising for surface functionalization.

■ ASSOCIATED CONTENT

Supporting Information

The Supporting Information is available free of charge on the ACS Publications website at DOI: 10.1021/acs.biomac.5b00951.

Additional ^{1}H, IG ^{13}C, DEPT, HSQC, NMR kinetics, MALDI-ToF and IR spectra as well as SEC elugrams (PDF)

■ AUTHOR INFORMATION

Corresponding Author

*E-mail: hfrey@uni-mainz.de.

Notes

The authors declare no competing financial interest.

■ ACKNOWLEDGMENTS

E.-M.C. thanks the Graduate School of Excellence Material Science in Mainz "MAINZ" for financial support and acknowledges technical assistance from Michael Bläser. Moreover, the authors want to thank Dr. Mihail Mondeshki for performing the solid state NMR experiments. Last but not least we thank Dr. Diana Knies for performing the MTT assay with HEK cells, Evelyn Montermann for performing the MTT assays with fibroblasts, the viability tests, as well as the transfection efficiency analysis and the adhesion assays, and Daniel Leibig and Tatjana Dänzer for preparing the internal control PS_{27}-(AGE)-$PE0_{130}$ for the adhesion assay. We thank Dr. Karl Fischer for performing the DLS measurements.

■ REFERENCES

(1) Vandenberg, E. J.; Mullis, J. C.; Juvet, R. S. *J. Polym. Sci., Part A: Polym. Chem.* **1989**, *27*, 3083−3112.
(2) Chen, Y.; Bednarek, M.; Kubisa, P.; Penczek, S. *J. Polym. Sci., Part A: Polym. Chem.* **2002**, *40*, 1991−2002.
(3) Schnell, H.; Neutwig, J.; Hintzmann, K.; Raichie, K.; Biedermann, W. US 2917468, U.S. Pat. Appl. Publ. Jan 1, 1956.
(4) Christ, E.-M.; Müller, S. S.; Berger-Nicoletti, E.; Frey, H. *J. Polym. Sci., Part A: Polym. Chem.* **2014**, *52*, 2850−2859.
(5) Tonhauser, C.; Wilms, D.; Korth, Y.; Frey, H.; Friedrich, C. *Macromol. Rapid Commun.* **2010**, *31*, 2127−2132.
(6) Schömer, M.; Schüll, C.; Frey, H. *J. Polym. Sci., Part A: Polym. Chem.* **2013**, *51*, 995−1019.
(7) Kim, Y. H.; Webster, O. W. *J. Am. Chem. Soc.* **1990**, *112*, 4592−4593.
(8) Zhou, Y.; Yan, D. *Angew. Chem., Int. Ed.* **2004**, *43*, 4896−4899.
(9) Jin, H.; Zheng, Y.; Liu, Y.; Cheng, H.; Zhou, Y.; Yan, D. *Angew. Chem., Int. Ed.* **2011**, *50*, 10352−10356.
(10) Zhou, Y.; Yan, D. *Chem. Commun.* **2009**, 1172−1188.
(11) Gao, C.; Yan, D. *Prog. Polym. Sci.* **2004**, *29*, 183−275.
(12) Zhou, Y.; Huang, W.; Liu, J.; Zhu, X.; Yan, D. *Adv. Mater.* **2010**, *22*, 4567−4590.
(13) Liu, Y.; Yu, C.; Jin, H.; Jiang, B.; Zhu, X.; Zhou, Y.; Lu, Z.; Yan, D. *J. Am. Chem. Soc.* **2013**, *135*, 4765−4770.
(14) Calderòn, M.; Quadir, M. A.; Sharma, S. K.; Haag, R. *Adv. Mater.* **2010**, *22*, 190−218.

DOI: 10.1021/acs.biomac.5b00951
Biomacromolecules 2015, 16, 3297−3307

(15) Dworak, A.; Walach, W.; Trzebicka, B. *Macromol. Chem. Phys.* **1995**, *196*, 1963−1970.
(16) Wilms, D.; Wurm, F.; Nieberle, J.; Böhm, P.; Kemmer-Jonas, U.; Frey, H. *Macromolecules* **2009**, *42*, 3230−3236.
(17) Sunder, A.; Hanselmann, R.; Frey, H.; Mülhaupt, R. *Macromolecules* **1999**, *32*, 4240−4246.
(18) Wilms, D.; Stiriba, S.-E.; Frey, H. *Acc. Chem. Res.* **2010**, *43*, 129−141.
(19) Moore, E.; Delalat, B.; Vasani, R.; Thissen, H.; Voelcker, N. H. *Biomacromolecules* **2014**, *15*, 2735−2743.
(20) Vandenberg, E. J. *J. Polym. Sci., Polym. Chem. Ed.* **1985**, *23*, 915−949.
(21) Kainthan, R. K.; Janzen, J.; Levin, E.; Devine, D. V.; Brooks, D. E. *Biomacromolecules* **2006**, *7*, 703−709.
(22) Wilms, D.; Stiriba, S.-E.; Frey, H. *Acc. Chem. Res.* **2010**, *43*, 129−141.
(23) Bednarek, M.; Biedron, T.; Helinski, J.; Kaluzynski, K.; Kubisa, P.; Penczek, S. *Macromol. Rapid Commun.* **1999**, *20*, 369−372.
(24) Magnusson, H.; Malmström, E.; Hult, A. *Macromol. Rapid Commun.* **1999**, *20*, 453−457.
(25) Bednarek, M.; Kubisa, P.; Penczek, S. *Macromolecules* **2001**, *34*, 5112−5119.
(26) Magnusson, H.; Malmström, E.; Hult, A. *Macromolecules* **2001**, *34*, 5786−5791.
(27) Mai, Y.; Zhou, Y.; Yan, D.; Lu, H. *Macromolecules* **2003**, *36*, 9667−9669.
(28) Saegusa, T.; Hashimoto, Y.; Matsumoto, S. *Macromolecules* **1971**, *4*, 1−3.
(29) Schüler, F.; Kerscher, B.; Beckert, F.; Thomann, R.; Mülhaupt, R. *Angew. Chem., Int. Ed.* **2013**, *52*, 455−458.
(30) Schadt, K.; Kerscher, B.; Thomann, R.; Mülhaupt, R. *Macromolecules* **2013**, *46*, 4799−4804.
(31) Kerscher, B.; Appel, A.-K.; Thomann, R.; Mülhaupt, R. *Macromolecules* **2013**, *46*, 4395−4402.
(32) Zhou, Y.; Huang, W.; Liu, J.; Zhu, X.; Yan, D. *Adv. Mater.* **2010**, *22*, 4567−4590.
(33) Appel, A.-K.; Thomann, R.; Mülhaupt, R. *Macromol. Rapid Commun.* **2013**, *34*, 1249−1255.
(34) Yu, S.; Dong, R.; Chen, J.; Chen, F.; Jiang, W.; Zhou, Y.; Zhu, X.; Yan, D. *Biomacromolecules* **2014**, *15*, 1828−1836.
(35) Xu, Y.; Gao, C.; Kong, H.; Yan, D.; Luo, P.; Li, W.; Mai, Y. *Macromolecules* **2004**, *37*, 6264−6267.
(36) Yan, D. *Science* **2004**, *303*, 65−67.
(37) Rahm, M.; Westlund, R.; Eldsäter, C.; Malmström, E. *J. Polym. Sci., Part A: Polym. Chem.* **2009**, *47*, 6191−6200.
(38) Zolotarskaya, O. Y.; Wynne, K. J.;Yang, H. *Society for Biomaterials, Proceedings* 2014, Abstract #819.
(39) Bednarek, M. *Polym. Int.* **2003**, *52*, 1595−1599.
(40) Parris, J. M.; Marchessault, R. H.; Vandenberg, E. J.; Mullis, J. C. *J. Polym. Sci., Part B: Polym. Phys.* **1994**, *32*, 749−758.
(41) Schömer, M.; Schüll, C.; Frey, H. *J. Polym. Sci., Part A: Polym. Chem.* **2013**, *51*, 995−1019.
(42) Magnusson, H.; Malmström, E.; Hult, A.; Johansson, M. *Polymer* **2002**, *43*, 301−306.
(43) Bednarek, M.; Kubisa, P. *J. Polym. Sci., Part A: Polym. Chem.* **2004**, *42*, 245−252.
(44) Schüll, C.; Nuhn, L.; Mangold, C.; Christ, E.; Zentel, R.; Frey, H. *Macromolecules* **2012**, *45*, 5901−5910.
(45) Xia, Y.; Wang, Y.; Wang, Y.; Wang, D.; Deng, H.; Zhuang, Y.; Yan, D.; Zhu, B.; Zhu, X. *Macromol. Chem. Phys.* **2011**, *212*, 1056−1062.
(46) Eigenmann, H. K.; Golden, D. M.; Benson, S. W. *J. Phys. Chem.* **1973**, *77*, 1687−1691.
(47) Burkhard, J. A.; Wuitschik, G.; Rogers-Evans, M.; Müller, K.; Carreira, E. M. *Angew. Chem.* **2010**, *122*, 9236−9251.
(48) Magnusson, H.; Malmström, E.; Hult, A.; Johansson, M. *Polymer* **2002**, *43*, 301−306.
(49) Schömer, M.; Seiwert, J.; Frey, H. *ACS Macro Lett.* **2012**, *1*, 888−891.
(50) Wynne, K. J.; Chakrabarty, S.; Zhang, W.; Chakravorty, A.; Oyesanya, O. O. US 20130183262, U.S. Pat. Appl. Publ. Jul 18, 2013.
(51) Sharma, K.; Zolotarskaya, O. Y.; Wynne, K. J.; Yang, H. *J. Bioact. Compat. Polym.* **2012**, *27*, 525−539.
(52) Zolotarskaya, O. Y.; Wagner, A. F.; Beckta, J. M.; Valerie, K.; Wynne, K. J.; Yang, H. *Mol. Pharmaceutics* **2012**, *9*, 3403−3408.
(53) Fritz, T.; Hirsch, M.; Richter, F. C.; Müller, S. S.; Hofmann, A. M.; Rusitzka, K. A. K.; Markl, J.; Massing, U.; Frey, H.; Helm, M. *Biomacromolecules* **2014**, *15*, 2440−2448.
(54) Schüll, C.; Gieshoff, T.; Frey, H. *Polym. Chem.* **2013**, *4*, 4730−4736.
(55) Rauscher, H.; Perucca, M.; Buyle, G. *Plasma Technology for Hyperfunctional Surfaces: Food, Biomedical and Textile Applications*; Wiley-VCH GmbH & CoGaA: Weinheim, 2010; p 211.
(56) Tonhauser, C.; Golriz, A. A.; Moers, C.; Klein, R.; Butt, H.-J.; Frey, H. *Adv. Mater.* **2012**, *24*, 5559−5563.
(57) Wang, D.; Zhao, T.; Zhu, X.; Yan, D.; Wang, W. *Chem. Soc. Rev.* **2015**, *44*, 4023−4071.
(58) Zheng, Y.; Li, S.; Weng, Z.; Gao, C. *Chem. Soc. Rev.* **2015**, *44*, 4091−4130.
(59) Pazos, J. F. US 5563221 A, U.S. Pat. Appl. Publ. Jan 1, 1995.
(60) Ionescu, M. *Chemistry and Technology of Polyols for Polyurethanes*; Rapra Technology limited: Shawbury, Shrewsbury, Shropshire, SY4 4NR, UK, 2005, 103.
(61) Tokar, R.; Kubisa, P.; Penczek, S.; Dworak, A. *Macromolecules* **1994**, *27*, 320−322.
(62) Perevyazko, I.; Seiwert, J.; Schömer, M.; Frey, H.; Schubert, U. S.; Pavlov, G. M. *Macromolecules* **2015**, *48* (16), 5887−5898.
(63) Kubisa, P.; Vairon, J. P. *Polymer Science: A Comprehensive Reference*; Matyjaszewski, K., Möller, M., Eds.; Elsevier BV: Amsterdam, 2012; Vol. *4*, pp 183−211.
(64) Hofmann, A. M.; Wurm, F.; Frey, H. *Macromolecules* **2011**, *44*, 4648−4657.

DOI: 10.1021/acs.biomac.5b00951
Biomacromolecules 2015, 16, 3297−3307